

Coherent pion production by neutrino scattering off nuclei

A. Kartavtsev* and E. A. Paschos†

Universität Dortmund, Institut für Physik, D-44221 Dortmund, Germany

G. J. Gounaris‡

Department of Theoretical Physics, Aristotle University of Thessaloniki, Gr-54124 Thessaloniki, Greece
(Received 7 December 2005; revised manuscript received 28 June 2006; published 7 September 2006)

The main part of coherent pion production by neutrinos on nuclei is essentially determined by partial conservation of the axial current (PCAC), provided that the leptonic momentum transferred square Q^2 remains sufficiently small. We give the formulas for the charged and neutral current cross sections, including also the small non-PCAC transverse current contributions and taking into account the effect of the μ^- -mass. Our results are compared with the experimental ones and other theoretical treatments.

DOI: [10.1103/PhysRevD.74.054007](https://doi.org/10.1103/PhysRevD.74.054007)

PACS numbers: 13.60.Le, 13.15.+g

I. INTRODUCTION

Coherent production of pions by neutrinos has been studied by many experimental groups and measurements have been made for neutrino energies ranging from 2 to 80 GeV [1–8]. The main characteristics of such cross sections are that the energy of the recoiling nucleus and the invariant momentum transfer to it, always remain very small. A characteristic signature of these events is a sharp peak in the low $|t|$ region. In addition to this, all experiments have observed that the momentum transfer from the leptonic sector Q^2 also remains very small, sharply peaking at $Q^2 \lesssim 0.2 \text{ GeV}^2$; while the dependence of the cross section on the neutrino energy appears logarithmic at high energies.

However, problems with the existence of the coherence phenomenon might appear at the lower energies used for the new oscillation experiments K2K, MiniBoone, MINOS etc. In particular, a new measurement by the K2K group at an average neutrino energy $E_1 = 1.3 \text{ GeV}$, has set an upper bound on the coherent pion production by neutrinos, which is far below the theoretical expectations [9]. This has raised questions on how accurately the coherent cross section can be calculated in such a low energy region, and whether detail event distributions may be predicted.

Theoretical calculations on the other hand, have presented general arguments based on the partial conservation of the axial current (PCAC) and the dominance of the axial current by pions or axial-vector mesons [10,11], or more complicated structures [12–15], occasionally using nuclear physics models [16]. The situation is not yet settled.

In some models one starts with the Adler relation [17] in the $Q^2 = 0$ limit and extrapolates it to small Q^2 values. In the work of Rein and Sehgal [10] the pole due to the $a_1(1260)$ resonance is introduced together with other assumptions for estimating the pion-nucleus cross section. In

several articles, Kopeliovich *et al.* [13] have claimed that the pion pole term acting on the leptonic current gives a small contribution proportional to the lepton mass, and they are led to argue that the axial current must be dominated by heavy meson fluctuation like $a_1(1260)$ or the $\rho\pi$ branch point.

Instead, we show here that a careful PCAC treatment determines the dominant terms in a unique way. More specifically, we decompose the leptonic current contribution into a spin = 0 and spin = 1 state with three helicity components. The inner product of the helicity zero polarization vector with the axial hadronic current leads to matrix elements in the $Q^2 \ll \nu^2$ region, determined by PCAC as $f_\pi T(\pi N \rightarrow \pi N)$, with T being the amplitude for the coherent pion-nucleus scattering, which is a smooth function of Q^2 , having no pion pole. This way, a Goldberger-Treiman-type relation is obtained, determining the true dominant contribution to coherent neutrino-pion production. In addition to this, there exist of course contributions arising from the transverse (off shell) vector and axial states, which are estimated phenomenologically and turn out to be very small.

Since the kinematics for the charged current (CC) cross sections obey $Q_{\min}^2 \sim m_\mu^2 \sim m_\pi^2$, all mass terms are retained in the calculation of the density matrix of the leptonic current and the phase space. For the neutral current (NC) reactions, the neutrino masses are of course negligible and the formulae are simplified. Using these, we plot $d\sigma/dQ^2$ for NC and CC pion production at small Q^2 , and compare the results.

The purpose of the present paper is to contribute in clarifying the theoretical framework for coherent pion production processes. More explicitly, we show that for energies of the produced pion above a few GeV, the main contribution to the coherent neutrino-pion production is determined by PCAC and the pion-Nucleus coherent scattering data. The remaining contributions arising from transverse off-shell vector and axial mesons, must always be very small. In particular, the transverse vector contribution is expressed in terms of the π^0 coherent photoproduc-

*Electronic address: akartavt@het.physik.uni-dortmund.de†Electronic address: paschos@physik.uni-dortmund.de‡Electronic address: gounaris@physics.auth.gr

tion data, and it is thus reliably estimated. Estimating the axial transverse contribution is more difficult, but a Regge analysis indicates that it should be comparable or probably smaller than the transverse vector contribution.

In the following, we present in Sec. II the general formalism for coherent π^\pm or π^0 production through neutrino scattering off a nucleus. In Sec. III we describe the experimental data and present our numerical results. The conclusions appear in Sec. IV.

II. THE FORMALISM

For clarity, we first concentrate on the π^+ production process through coherent ν_μ scattering off a heavy nucleus N , according to the process

$$\nu_\mu(k_1)N(P) \rightarrow \mu^-(k_2)\pi^+(p_\pi)N(P'), \quad (1)$$

where the momenta are indicated in parentheses. Here $q = k_1 - k_2$ is the momentum four-vector transferred from the leptonic current to the nucleus N , so that its energy-component $\nu = q_0 = E_1 - E_2$ (with E_1 and E_2 being the ν_μ and μ^- laboratory energies, respectively) denotes the energy given by the current to the π^+N -pair in the Lab frame.

In the coherent scattering regime the nucleus spin is not flipped, and its recoil must be minimal, so that $\nu \simeq E_\pi$, with E_π being the pion energy in the laboratory frame. The existing experimental data also suggest that in the coherence regime $0 \leq Q^2 = -q^2 \lesssim 0.2 \text{ GeV}^2$, and that the squared momentum-transfer in the hadronic system $t = (q - p_\pi)^2 = (P - P')^2$ is peaked at very small values.

The invariant amplitude for the process (1) may be written as

$$T_W = -\frac{G_F V_{ud}}{\sqrt{2}} \bar{u}(k_2) \gamma^\rho (1 - \gamma_5) u(k_1) (\mathcal{V}_\rho^+ - \mathcal{A}_\rho^+), \quad (2)$$

where the first factor gives the $(\nu_\mu \rightarrow \mu)$ -matrix element of the leptonic current, while

$$\begin{aligned} \mathcal{V}_\rho^+ &= \langle \pi^+ N | V_\rho^1 + iV_\rho^2 | N \rangle, \\ \mathcal{A}_\rho^+ &= \langle \pi^+ N | A_\rho^1 + iA_\rho^2 | N \rangle, \end{aligned} \quad (3)$$

describe (in momentum space) the hadronic matrix elements of the charged vector and axial currents, respectively. V_{ud} in (2) denotes the appropriate Cabibbo-Kobayashi-Maskawa quark-mixing matrix (CKM) element.

Since, the charged leptonic current is not conserved ($m_\mu \neq 0$), it contains spin = 0 degrees of freedom described by its component along the vector

$$\epsilon_l^\rho = \frac{q^\rho}{\sqrt{Q^2}}, \quad (4)$$

as well as spin = 1 degrees of freedom describing off-shell gauge bosons with the helicity polarization vectors

$$\begin{aligned} \epsilon^\rho(\lambda = \pm 1) &= \mp \begin{pmatrix} 0 \\ 1 \\ \pm i \\ 0 \end{pmatrix}^\rho, \\ \epsilon^\rho(\lambda = 0) &= \frac{1}{\sqrt{Q^2}} \begin{pmatrix} |\vec{q}| \\ 0 \\ 0 \\ q_0 \end{pmatrix}^\rho, \end{aligned} \quad (5)$$

when \vec{q} is taken along the \hat{z} -axis. The $\lambda = \mp 1$ polarizations in (5) are often denoted as $L(R)$ respectively, the vanishing helicity vector $\epsilon^\rho(\lambda = 0)$ is identical to ϵ_S^ρ of [18], and $\epsilon^\rho(\lambda)q_\rho = 0$ is of course always satisfied.

Anticipating that we later integrate over all relative angles between the (\vec{k}_1, \vec{k}_2) -leptonic plane and the (\vec{q}, \vec{p}_π) pion production plane, the only density matrix elements needed for the above spin = 0 and 1 states hitting the nucleus N are [19]

$$\begin{aligned} \frac{(\tilde{L}_{RR} + \tilde{L}_{LL})}{2} &= Q^2 \left[1 + \frac{(2E_1 - \nu)^2}{\vec{q}^2} \right] - \frac{m_\mu^2}{\vec{q}^2} [2\nu(2E_1 - \nu) + m_\mu^2], & \frac{(\tilde{L}_{RR} - \tilde{L}_{LL})}{2} &= -\frac{2[Q^2(2E_1 - \nu) - \nu m_\mu^2]}{|\vec{q}|}, \\ \tilde{L}_{00} &= \frac{2[Q^2(2E_1 - \nu) - \nu m_\mu^2]^2}{Q^2 \vec{q}^2} - 2(Q^2 + m_\mu^2), & \tilde{L}_{ll} &= 2m_\mu^2 \left(\frac{m_\mu^2}{Q^2} + 1 \right), & \tilde{L}_{l0} &= \frac{2m_\mu^2 [Q^2(2E_1 - \nu) - \nu m_\mu^2]}{Q^2 |\vec{q}|}. \end{aligned} \quad (6)$$

Using these and the hadronic current elements in (3), the square of the amplitude in (2), summed over all μ^- polarizations, is written as

$$\begin{aligned}
|\overline{T_W}|^2 = & G_F^2 |V_{ud}|^2 \left\{ \frac{(\tilde{L}_{RR} + \tilde{L}_{LL})}{2} \sum_{\lambda=L,R} |(\mathcal{V}^+ - \mathcal{A}^+) \cdot \epsilon(\lambda)|^2 \right. \\
& + \frac{(\tilde{L}_{RR} - \tilde{L}_{LL})}{2} [|(\mathcal{V}^+ - \mathcal{A}^+) \cdot \epsilon(R)|^2 - |(\mathcal{V}^+ - \mathcal{A}^+) \cdot \epsilon(L)|^2] + \tilde{L}_{00} |(\mathcal{V}_\rho^+ - \mathcal{A}_\rho^+) \epsilon^\rho(\lambda=0)|^2 \\
& \left. + \frac{\tilde{L}_{ll}}{Q^2} |(\mathcal{V}_\rho^+ - \mathcal{A}_\rho^+) q^\rho|^2 + \frac{2\tilde{L}_{l0}}{\sqrt{Q^2}} \Re [(\mathcal{V}_\rho^+ - \mathcal{A}_\rho^+) \epsilon^\rho(0) \cdot [(\mathcal{V}_\mu^+ - \mathcal{A}_\mu^+) q^\mu]^*] \right\}, \quad (7)
\end{aligned}$$

where the first two terms may be interpreted as giving the contributions from the transverse spin = 1 components of the hadronic currents, the third term gives the helicity $\lambda = 0$ hadronic contribution, the fourth term arises from the spin = 0 component, and finally the last term from the interference of the latter two.

We first concentrate on the axial current matrix elements in the last three terms of (7), which turn out to give the most important contributions, for the GeV-scale kinematic region where coherence is relevant. The pion poles contained in these terms, induce a singularity at low Q^2 , which must be carefully separated, before any approximation is made.

To achieve this we note that the axial hadronic element in (3) consists of the pion pole contribution, and the rest we call \mathcal{R}^ρ , induced by $a_1(1260)$ and any other isovector axial meson that might exist. It is thus, written as

$$-i\mathcal{A}_\rho^+ = \frac{f_\pi \sqrt{2} q^\rho}{Q^2 + m_\pi^2} T(\pi^+ N \rightarrow \pi^+ N) - \mathcal{R}^\rho, \quad (8)$$

where $T(\pi^+ N \rightarrow \pi^+ N)$ is the π -nucleus purely hadronic invariant amplitude, $f_\pi \simeq 92$ MeV, and \mathcal{R}^ρ is a very smooth function of Q^2 whose dependence on it is ignored [20]. The usual PCAC treatment leads to

$$\begin{aligned}
-iq^\rho \mathcal{A}_\rho^+ &= \langle \pi^+ N | \partial^\rho A_\rho^+ | N \rangle \\
&= \frac{f_\pi m_\pi^2 \sqrt{2}}{Q^2 + m_\pi^2} T(\pi^+ N \rightarrow \pi^+ N) \\
&= -\frac{f_\pi Q^2 \sqrt{2}}{Q^2 + m_\pi^2} T(\pi^+ N \rightarrow \pi^+ N) - q_\mu \mathcal{R}^\mu, \quad (9)
\end{aligned}$$

$$\Rightarrow q^\mu \mathcal{R}_\mu = -f_\pi \sqrt{2} T(\pi^+ N \rightarrow \pi^+ N). \quad (10)$$

It is amusing to emphasize that (10) is strongly reminiscent of the classical Goldberger-Treiman treatment, where the pion pole not only determines $\partial^\mu A_\mu$, but in fact also the complete axial current coupling [21].

Using now (8), and $\epsilon(0)_\rho q^\rho = 0$ implied by (4) and (5), we conclude

$$\epsilon(0)^\rho \mathcal{A}_\rho^+ = -i\epsilon(0)^\rho \mathcal{R}_\rho \simeq i \frac{f_\pi \sqrt{2}}{\sqrt{Q^2}} T(\pi^+ N \rightarrow \pi^+ N), \quad (11)$$

where in the first step the pion pole contribution vanishes identically, while the last step is due to the smoothness of \mathcal{R}^ρ and the restriction to $\nu \gg \sqrt{Q^2}$, which justify the approximation

$$\nu \gg \sqrt{Q^2} \Rightarrow \epsilon^\rho(0) \simeq q^\rho / \sqrt{Q^2}. \quad (12)$$

In order for the simple pion dominating picture obtained below to be valid, the kinematics should always be chosen such that $\nu \gg \sqrt{Q^2}$. To guarantee this we introduce the parameter ξ in (A7) of the appendix.

Since (11) is our most important theoretical result, it might be worth emphasizing that it would be incorrect to apply the approximation (12) directly on the $\epsilon(0)^\rho \mathcal{A}_\rho^+$ computation using (8), because that will replace the identically vanishing expression $\epsilon^\mu(0) q_\mu / (Q^2 + m_\pi^2)$, by the nonvanishing and in fact large quantity $-\sqrt{Q^2} / (Q^2 + m_\pi^2)$ [22].

The relations (9) and (11) fully determine the axial current contribution to the last three terms of (7). We also remark that these results are consistent with the Adler theorem in the parallel lepton configuration [17,23], provided we set $m_\mu = 0$.

Furthermore, the vector hadronic elements in the last three terms of (7) give no contribution; since the vector current is conserved, and the applicability of (12) for calculating $\epsilon^\rho(\lambda=0) \mathcal{V}_\rho^+$ is guaranteed by the absence of any low mass singularity. Moreover, since in the coherence regime there is no $R - L$ polarization sensitivity to the vector or axial-vector boson cross sections, there will not be any contribution from the second term in (7).

Thus, the CC neutrino coherent pion production cross section off a nucleus N becomes

$$\begin{aligned}
\frac{d\sigma(\nu N \rightarrow \mu^- \pi^+ N)}{dQ^2 dv dt} = & \frac{G_F^2 |V_{ud}|^2 \nu}{2(2\pi)^2 E_1^2} \left\{ \frac{f_\pi^2}{Q^2} \left[\tilde{L}_{00} + \tilde{L}_{ll} \left(\frac{m_\pi^2}{Q^2 + m_\pi^2} \right)^2 + 2\tilde{L}_{l0} \frac{m_\pi^2}{Q^2 + m_\pi^2} \right] \frac{d\sigma(\pi^+ N \rightarrow \pi^+ N)}{dt} \right. \\
& \left. + \frac{(\tilde{L}_{RR} + \tilde{L}_{LL})}{2} \left[\frac{1}{2\pi\alpha} \frac{d\sigma(\gamma N \rightarrow \pi^0 N)}{dt} + \frac{d\sigma(A_T^+ N \rightarrow \pi^+ N)}{dt} \right] \right\}, \quad (13)
\end{aligned}$$

expressed in terms of the leptonic density matrix elements in (6). In deriving this expression we have integrated over all angles between the lepton- and (\vec{q}, \vec{p}_π) -planes, and ignored any vector-axial interference in (7), since it will anyway cancel out after the t -integration we do, before comparing to the experimental data. Notice that in contrast to (7), the presentation in (13) first gives the numerically most important terms arising from the $\lambda = 0$ and the spin = 0 components of the leptonic current, and then the less important contributions from its transverse vector and axial components.

In treating the phase space in (13) we have used

$$\begin{aligned} W^2 &\equiv (q + P)^2 = M_N^2 - Q^2 + 2M_N\nu \simeq M_N^2 + 2M_N\nu \\ &\simeq M_N^2 + 2M_N E_\pi, \end{aligned} \quad (14)$$

for the invariant mass-squared of the π^+N -pair. Thus, the three differential cross sections occurring in the right-hand side of (13) should be thought as functions of t , and the laboratory energy $\nu \simeq E_\pi$, of the particle hitting the nucleus.

We next turn to the last two terms within the curly brackets in (13), which are induced by the transverse components of all off-shell vector and axial-vector mesons coupled to the \mathcal{V}_ν^+ and \mathcal{A}_ν^+ matrix elements at very small

Q^2 ; compare (3). The vector term is directly related, (after an isospin rotation producing a factor 2), to π^0 photo-production for unpolarized photons. In deriving this, it is important to realize that the isoscalar part of the electromagnetic current does not contribute to the coherent π^0 amplitude. This contribution is estimated in the next section, using the experimental data [24].

The transverse axial term within the curly brackets in (13)

$$\frac{d\sigma(A_T^+ N \rightarrow \pi^+ N)}{dt} = \frac{\sum_{\lambda=L,R} |\mathcal{A}^+ \cdot \epsilon(\lambda)|^2}{128\pi\nu^2 M_N^2}, \quad (15)$$

expressed in terms of the axial matrix element of (3), describes the cross section for π^+ -production through ‘‘transversely polarized charged axial currents’’. To calculate it, we would need to know all possible a_1^+ (1260)-type mesons that couple to the axial current, their couplings to it, and the corresponding $\sigma(a_{1T}^+ N \rightarrow \pi^+ N)$ off-shell transverse a_1 cross sections, at very small Q^2 . We estimate this also in the next section.

A similar procedure may be carried out for the NC coherent π^0 -production, for which the result

$$\begin{aligned} \frac{d\sigma(\nu N \rightarrow \nu \pi^0 N)}{dQ^2 d\nu dt} &= \frac{G_F^2 \nu}{4(2\pi)^2 E_1^2} \left\{ \frac{f_\pi^2}{Q^2} \tilde{L}_{00} \frac{d\sigma(\pi^+ N \rightarrow \pi^+ N)}{dt} + \frac{(\tilde{L}_{RR} + \tilde{L}_{LL})}{2} \left[\frac{(1 - 2s_W^2)^2}{2\pi\alpha} \frac{d\sigma(\gamma N \rightarrow \pi^0 N)}{dt} \right. \right. \\ &\quad \left. \left. + \frac{d\sigma(A_T^+ N \rightarrow \pi^+ N)}{dt} \right] \right\} \end{aligned} \quad (16)$$

is found, provided the assumption

$$\frac{d\sigma(\pi^+ N \rightarrow \pi^+ N)}{dt} \simeq \frac{d\sigma(\pi^0 N \rightarrow \pi^0 N)}{dt}, \quad (17)$$

is made, which is on the same footing as the isospin rotation we used in writing (13) in terms of the π^0 photo-production data.

In (16), the leptonic density matrix elements are given by the same expressions as in (6), with the obvious substitution $m_\mu \rightarrow 0$. Comparing the NC result (16), to the CC in (13), we see that there is no CKM factor now, and that the axial contribution to the NC cross section is a factor 2 smaller than the CC one. For the vector contribution though, an extra reduction by a factor $(1 - 2s_W^2)^2$ appears, which is due to the fact that Z couples not only to the $SU_L(2)$ -current, but also to the isovector part of the electromagnetic current.

III. NUMERICAL ESTIMATES AND RESULTS

For numerical estimates we must calculate the three cross sections appearing in Eqs. (13) and (16). The dominant contribution comes from $\sigma(\pi^+ N \rightarrow \pi^+ N)$, for which

we use data on coherent scattering of pions on nuclei. This being the dominant term, we calculate it precisely and present the results in the figures below. The other two cross sections involve coherent photoproduction of pions and the $A_T^+ N \rightarrow \pi^+ N$ process, where the axial-vector particles are transversely polarized and give smaller contributions. We have estimated them using available data and showed that they are very small. Thus, assigning to the latter two cross section an uncertainty even as large as 50% does not affect our results.

For isoscalar targets, like C^{12} , O^{16} . . . , isospin symmetry implies $d\sigma(\pi^+ N) \simeq d\sigma(\pi^- N) \simeq d\sigma(\pi^0 N)$. In the actual calculation we use the coherent pion-carbon scattering data [25], with additional data being available on other nuclei and other energies in [26,27]. Data from other nuclei are normalized to carbon, using the A -dependence law $A^{2/3}$, observed in hadronic experiments [28] and in pion photo-production [29].

In all cases, ν is identified with the laboratory pion energy, and the integration over t is done for the low values shown in the appendix. Thus, the pion-carbon cross section $d\sigma(\pi^+ C \rightarrow \pi^+ C)/dt$ is integrated from $|t|_{\min}$ given in (A2), to $|t|_{\max} \simeq 0.05 \text{ GeV}^2$ corresponding to the first dip

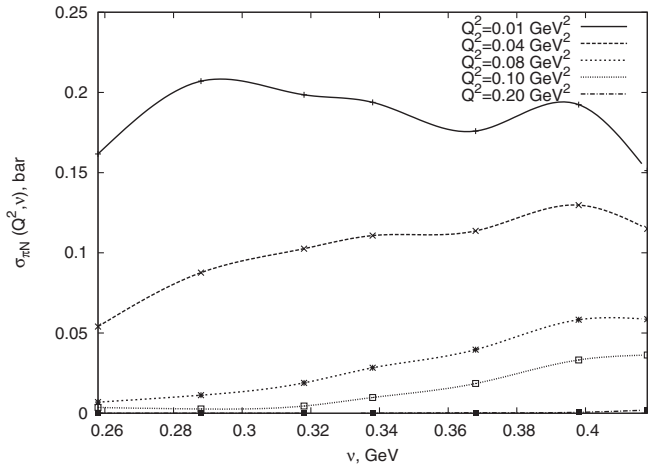


FIG. 1. Pion-carbon cross section integrated over t in the range discussed in the text, as a function of ν , at different values of Q^2 .

of the pion-carbon cross section. We checked that this t_{\min} is sufficiently large for the cross section to be outside the Coulomb peak which also contributes to the $\pi^\pm N$ scattering at very small angles [30]. The resulting integrals are functions of the pion energy ν , and the momentum transfer squared Q^2 , introduced through the lower limit of the t -integration. The results are shown in Fig. 1, for various ν and Q^2 values.

Integrating next (13) and (16) over ν in the range of (A7), we obtain the $\sigma(\pi^+ N \rightarrow \pi^+ N)$ contribution to the differential cross sections $d\sigma(\nu N \rightarrow \mu^- \pi^+ N)/dQ^2$ and $d\sigma(\nu N \rightarrow \nu \pi^0 N)/dQ^2$, for the CC and NC reactions depicted in Fig. 2. We notice that the shapes of the CC and the NC distributions are different, most notably because of the m_μ -mass effects. The results in Fig. 2 correspond to $\xi = 3$,

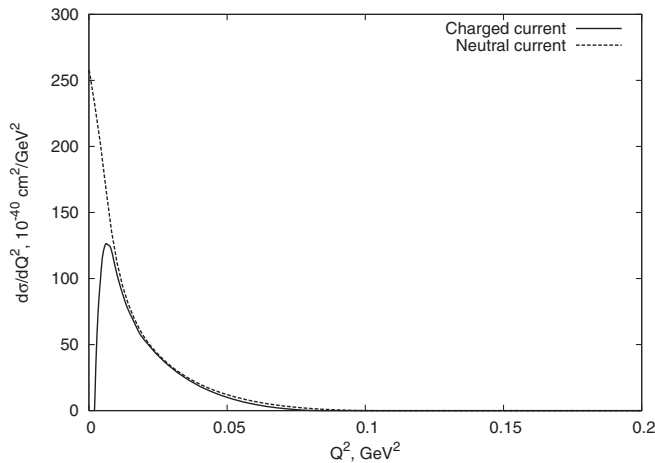


FIG. 2. The differential cross sections for the coherent pion production by neutrinos $d\sigma(\nu N \rightarrow \mu^- \pi^+ N)/dQ^2$ and $d\sigma(\nu N \rightarrow \nu \pi^0 N)/dQ^2$, for $E_1 = 1.0$ GeV. Only $\sigma(\pi^+ N \rightarrow \pi^+ N)$ has been taken into account, since the transverse vector and axial contribution are negligible. The curves correspond to $\xi = 3$; see (A7).

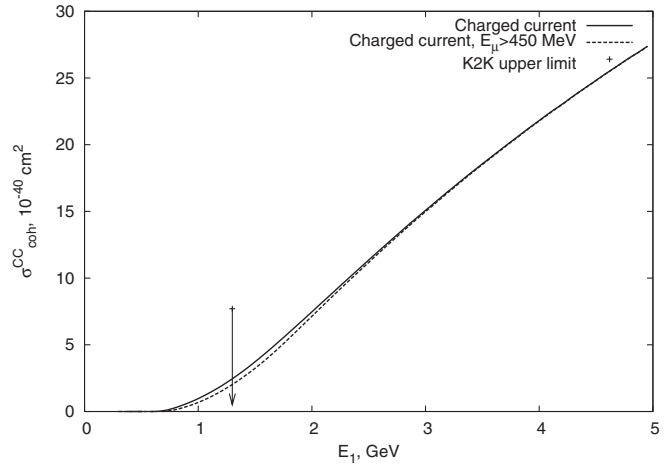


FIG. 3. Integrated cross section of the coherent pion production per carbon nucleus by neutrinos in the CC case. Only $\sigma(\pi^+ N \rightarrow \pi^+ N)$ has been taken into account, since the transverse vector and axial contribution are negligible. The upper bound is from K2K including 1 standard deviation. Dotted line represents integrated cross section with a threshold value for the muon energy $E_\mu > 450$ MeV. The theoretical curves correspond to $\xi = 3$; compare (A7).

defined in (A7), in order to be consistent with (12). We also note that such shape differences as indicated in Fig. 2, must be taken into account, in the comparison with the Adler parallel configuration.

Finally, integrating over Q^2 in the region (A9), we obtain the results in Fig. 3 and 4.

We next turn to the transverse vector and axial contributions supplying the terms proportional to the density

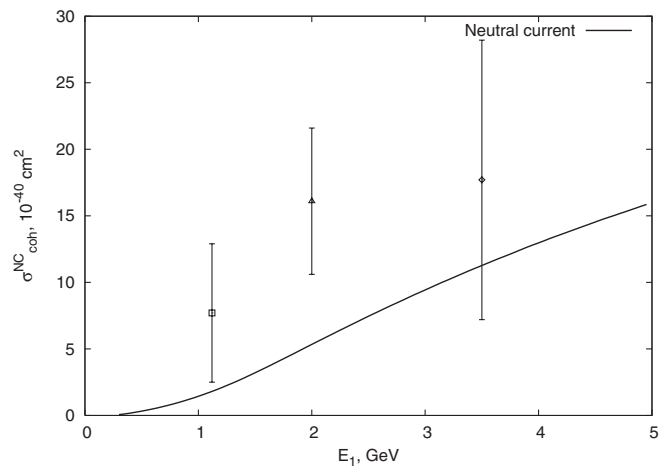


FIG. 4. Integrated cross section of the coherent pion production per carbon nucleus by neutrinos in the NC case. Only $\sigma(\pi^+ N \rightarrow \pi^+ N)$ has been taken into account, since the transverse vector and axial contribution are negligible. The experimental points for NC are from: \square MiniBoone [40], \triangle Aachen-Padova [1], \diamond Gargamelle [3]. The theoretical curve corresponds to $\xi = 3$.

matrix elements $\tilde{L}_{RR} + \tilde{L}_{LL}$ in (13) and (16). For the photon induced reaction, there exist data on the photo-production of mesons off nuclei [24,29,31]. The A -dependence reported in [29] is $A^{2/3}$ which indicates that the same shadowing as in π -nucleus interactions takes place. Using then data on Pb from Fig. 9 of [24] at $E_\gamma = 200\text{--}350$ MeV, and integrating them over the first peak, we obtain

$$\frac{1}{2\pi\alpha} \int_{|t_{\min}|}^{0.01 \text{ GeV}^2} dt \frac{d\sigma(\gamma N \rightarrow \pi^0 N)}{dt} \left(\frac{12}{207}\right)^{2/3} \simeq 1.40 \text{ mb}, \quad (18)$$

where the factor $1/2\pi\alpha$ comes from the elimination of the electromagnetic coupling, and $(12/207)^{2/3}$ from changing the cross section from lead to carbon. The numerical value in (18) should be compared with the upper most curve in our Fig. 1. We note that the transverse vector current contribution is approximately 1%, of the pion contribution. In addition to it, the ratio of their coefficients in (13), $(\tilde{L}_{RR} + \tilde{L}_{LL})/2$ to $f_\pi^2[\tilde{L}_{00} + \dots]/Q^2$ in the interesting kinematic region is ~ 0.2 . We conclude therefore, that the transverse vector-current contribution to (13) and (16) is negligible, compared to the pion contribution.

Estimates of the transverse axial current contribution at low energies are more difficult, because of the absence of data. However, as argued below, this contribution to (13) and (16) should be very small and probably smaller than the transverse vector one.

A very rough estimate for (15) may be obtained by assuming that it receives important contributions from the a_1^+ (1260) resonance. We need two kinds of measurements for this. The first is the partial τ^- -width $\Gamma(\tau^- \rightarrow a_1^- \nu_\tau)$, which determines the a_1 coupling to the axial current f_{a_1} , defined through [compare (3)]

$$\langle 0 | A_\rho^1 + iA_\rho^2 | a_1^+ \rangle = \frac{m_{a_1}^2}{f_{a_1}} \epsilon_\rho(a_1), \quad (19)$$

using

$$\Gamma(\tau^- \rightarrow a_1^- \nu_\tau) = \frac{G_F^2 m_{a_1}^2 m_\tau^3}{16\pi f_{a_1}^2} \left(1 - \frac{m_{a_1}^2}{m_\tau^2}\right)^2 \left(1 + \frac{2m_{a_1}^2}{m_\tau^2}\right), \quad (20)$$

where $(m_{a_1}, \epsilon_\rho(a_1))$ are the a_1 mass and polarization vector, and m_τ is the τ mass. Unfortunately the data for $\tau^- \rightarrow a_1^- \nu_\tau$ do not show a clear 3π resonant state.

Using as an alternative the corresponding coupling of the ρ -meson to the isovector current $f_\rho^2 \simeq 32$, determined from e.g. the $\Gamma(\rho^0 \rightarrow e^- e^+)$ data, and taking into account the fact that the a_1 -coupling to the axial current could not be stronger [32], we expect

$$f_{a_1}^2 \gtrsim 32. \quad (21)$$

If in addition some data on $d\sigma(\pi^\pm N \rightarrow a_{1T}^\pm N)/dt$ for transverse a_1 production were available, we would estimate

$$\frac{d\sigma(A_T^+ N \rightarrow \pi^+ N)}{dt} \sim \frac{2}{f_{a_1}^2} \frac{d\sigma(\pi^+ N \rightarrow a_{1T}^+ N)}{dt}, \quad (22)$$

where the laboratory energy of the incident pion is again identified with ν .

To get a feeling of the relative magnitude of the transverse axial versus transverse vector contribution, we compare the integrated $\pi^- p \rightarrow a_1^- p$ data at $E_\pi = 16$ GeV of [33], to the $\gamma p \rightarrow \pi^0 p$ data at $E_\gamma = 6$ GeV of [34].

The integrated diffractive cross section found in [33] at $E_\pi = 16$ GeV is $\sigma(\pi^- p \rightarrow a_1^- p) = 250 \pm 50 \mu\text{b}$. Most of this is of course helicity conserving and refers to the production of a_1 with vanishing helicity. According to the authors estimate [33], the transverse helicity part constitutes a fraction of 0.16 ± 0.08 of this. Substituting this in (22), using (21), we find

$$\sigma(A_T^- p \rightarrow \pi^- p) \lesssim 2.5 \pm 1.2 \mu\text{b}, \quad (23)$$

which should be compared with the transverse vector contribution [34,35]

$$\frac{1}{2\pi\alpha} \sigma(\gamma p \rightarrow \pi^0 p) \simeq 5 \mu\text{b} \quad \text{at } E_\gamma = 6 \text{ GeV}. \quad (24)$$

In comparing (23) and (24) we should remember that the transverse vector and axial processes in (13), are both determined by helicity-flip amplitudes. But in contrast to the ω -Regge trajectory which contributes uninhibited to the coherent vector amplitude [10], the only established Regge singularity that can contribute to the coherent axial amplitude would have been the Pomeron, provided the associate a_1 -particles had helicity zero. Since the currents we consider are transverse though, the only possible contributions to the axial amplitude arise either from the small s -channel helicity violating component of the Pomeron [36,37] or the generally unimportant σ -trajectory. On the basis of these, we conclude that (23) is very likely an overestimate. For coherent production on a carbon target, we must scale up the proton estimates (23) and (24) by a factor $12^{2/3} \simeq 5.2$, so that they always remain very small in comparison to the pion-carbon coherent result that we plotted as the uppermost curve in the Fig. 1.

To sum up, the limited amount of data forced us to use phenomenological estimates which imply that the transverse contributions are very small in comparison to the pion term. Our results in Figs. 1–4, based on the pion-nucleus data only, can be considered as lower bounds, with the actual cross sections being a few percent above them.

We turn next to the implications for the oscillation experiments. Figure 3 shows our results for CC coherent contribution to neutrino-pion production $\sigma_{\text{coh}}^{CC}(E_1)$ for $\nu \geq \xi\sqrt{Q^2}$ for $\xi = 3$. The value of $\xi = 3$ is chosen so that

condition (12) is satisfied. The figure shows an almost linear increase with neutrino energies. We note that there is a rapid growth of the cross section, up to $E_1 \sim 5$ GeV. In fact at $E_1 = 2.0$ GeV the cross section is almost 3 times bigger than at 1.0 GeV. For $E_1 = 1.3$ GeV and $\xi = 3$, the predicted coherent CC cross section on carbon target is $\sigma_{\text{coh}}^{\text{CC}} = 2 \times 10^{-40}$ cm² with the $E_2 \equiv E_\mu > 450$ MeV cut applied.

Unfortunately there exist no experimental data that take into account the $\xi = 3$ -cut we have imposed for consistency with our approximation (12). The only existing data for coherent pion production on carbon [9]

$$\sigma_{\text{coh}}^{\text{CC}} \leq (7.7 \pm 1.6(\text{stat}) \pm 3.6(\text{sys})) \times 10^{-40} \text{ cm}^2 \quad (25)$$

are obtained by integrating over all ν -values larger than ν_{min} appearing in (A3), and therefore provide an upper bound to the value obtained when the $\xi = 3$ -cut is imposed. They are of course consistent with our result [38]

Finally, we apply our work to the coherent production of π^0 in neutral current reactions. This reaction is an important background in oscillation experiments searching for the oscillation of ν_μ 's to ν_e 's. Several oscillation experiments use two detectors with a long-base-line. The far away detector searches among other channels also for $\nu_e \rightarrow e^-$ interactions. The π^0 's produced via coherent scattering decay to two photons whose Cherenkov light mimics that of electrons. Furthermore, when the oscillation is to other types of active neutrinos all species contribute equally to coherent scattering, but only ν_e 's produce electrons through the charged current. Thus a good understanding of coherent π^0 production is very important.

The NC cross section is calculated from (16), assuming $\sigma(\pi^0 C \rightarrow \pi^0 C) \simeq \sigma(\pi^+ C \rightarrow \pi^+ C)$, which follows from isospin symmetry. The NC cross section is approximately half as big as the CC cross section. The result is shown in Fig. 4 with the solid curve again corresponding to $\xi = 3$. We plotted also three experimental points carried at three different energies and targets made of carbon, aluminum, and freon, respectively. We use carbon as our reference nucleus and scale the results for other nuclei by the $A^{2/3}$ rule, as we discussed earlier. Rescaling the Aachen and Gargamelle data, we obtain the points in Fig. 4. The three points have large errors and are consistent with the theoretical curves. As in the CC case, we should mention though that the $\xi = 3$ cut was not imposed in these data. Had this been done, the data would have been considerably reduced.

IV. CONCLUSIONS

We revisited in this article coherent pion production by neutrinos. There are several reasons for returning to this old topic. First there are new data which are becoming available and need an explanation. Second, we clarify the theoretical framework for the CC and NC cross section formulas (13) and (16). In doing this, we decompose the

leptonic tensor into density matrix elements keeping the muon mass. Then we showed that a careful application of PCAC leads to the formulas (13) and (16), where the bulk of the coherent neutrino-pion production is described by the coherent $\pi N \rightarrow \pi N$ scattering, provided Q^2 is sufficiently small and $\nu \gg \sqrt{Q^2}$. Only for such ν -values, we obtain the simple pion dominating picture presented in this paper.

A third contribution is the discussion of data and estimates for the cross sections. To this end we collected data for the coherent production of pions on nuclei with pion and photon incident beams. The relevant results for pion coherent scattering are shown in Fig. 1; while the photo-production contributions turned out to be very small. Collecting all terms together we computed the differential and integrated cross sections shown in Figs. 2–4, keeping the exact phase space.

The results in Fig. 2 demonstrate that a careful test of PCAC demands that we keep the muon mass terms and the correct phase space, because, by neglecting the muon mass the integrated charged current cross section is overestimated by a factor of 2. Corrections from the muon mass are also discussed in Ref. [39] and in the Adler recollections [17]. It will be important for future experiments that a cut like $\xi = 3$ is imposed, because only then is the validity of a PCAC treatment guaranteed. In any case, the integrated cross sections shown in Figs. 3 and 4 are in satisfactory agreement with experimental data, in view of the large experimental errors.

We feel that the analysis proposed in this article, together with the use of hadronic data, should provide accurate estimates for coherent pion production also at higher neutrino energies.

ACKNOWLEDGMENTS

E. A. P. wishes to thank Dr. A. Thomas and colleagues for their hospitality at Jefferson Laboratory where part of the work was done and Dr. A. Afanasev for stimulating discussions. The financial support of BMBF, Bonn under Contract No. 05HT 4 PEA/9 is gratefully acknowledged. A. K. wishes to thank the Graduiertenkolleg 841 ‘‘Physik der Elementarteilchen an Beschleunigern und im Universum’’ at University of Dortmund for financial support. In addition, G. J. G. would like to thank the colleagues of the Physics Department at the University of Dortmund for the hospitality they extended to him.

APPENDIX: KINEMATICS

In this appendix, we give the kinematic limits for the integration of the differential cross sections in (13) and (16).

The integration is organized by first performing the t -integral in the range

$$|t_{\text{min}}| < -t < 0.05 \text{ GeV}^2, \quad (\text{A1})$$

where

$$t_{\min} = \frac{(Q^2 + m_\pi^2)^2 - [\sqrt{\lambda(W^2, -Q^2, M_N^2)} - \sqrt{\lambda(W^2, m_\pi^2, M_N^2)}]^2}{4W^2} \simeq -\left(\frac{Q^2 + m_\pi^2}{2\nu}\right)^2, \quad (\text{A2})$$

where $\lambda(a, b, c) = a^2 + b^2 + c^2 - 2ab - 2ac - 2bc$ is used.

At fixed Q^2 and $s \equiv (k_1 + P)^2 = M_N^2 + 2M_N E_1$, the kinematical minimum and maximum ν -values are

$$\nu_{\min} = \frac{(W_{\min}^2 + Q^2 - M_N^2)}{2M_N}, \quad (\text{A3})$$

$$\nu_{\max} = \frac{(W_{\max}^2 + Q^2 - M_N^2)}{2M_N}, \quad (\text{A4})$$

where

$$W_{\min}^2 = (M_N + m_\pi)^2, \quad (\text{A5})$$

$$W_{\max}^2 = \left\{ \frac{1}{4} s^2 \left(1 - \frac{M_N^2}{s}\right)^2 \left(1 - \frac{m_\mu^2}{s}\right) - \left[Q^2 - \frac{s}{2} \left(1 - \frac{M_N^2}{s}\right) + \frac{m_\mu^2}{2} \left(1 + \frac{M_N^2}{s}\right) \right]^2 \right\} \times \left(1 - \frac{M_N^2}{s}\right)^{-1} (Q^2 + m_\mu^2)^{-1}. \quad (\text{A6})$$

To assure though that the condition for the validity of (12) is also satisfied, the ν -integration is done in the range

$$\max(\xi\sqrt{Q^2}, \nu_{\min}) < \nu < \nu_{\max}, \quad (\text{A7})$$

where for the present application we selected $\xi = 3$.

Finally, the kinematically allowed minimum Q^2 value is

$$Q^2 = \frac{(s - M_N^2)}{2} \left[1 - \lambda^{1/2} \left(1, \frac{m_\mu^2}{s}, \frac{W_{\min}^2}{s}\right) \right] - \frac{1}{2} \left[W_{\min}^2 + m_\mu^2 - \frac{M_N^2}{s} (W_{\min}^2 - m_\mu^2) \right] \quad (\text{A8})$$

where (A5) is used. The interesting Q^2 -region for coherent scattering then is

$$Q_{\min}^2 < Q^2 \lesssim 0.2 \text{ GeV}^2. \quad (\text{A9})$$

-
- [1] H. Faissner *et al.*, Phys. Lett. **125B**, 230 (1983).
[2] P. Marage *et al.* (WA59), Phys. Lett. **140B**, 137 (1984).
[3] E. Isiksal, D. Rein, and J. G. Morfin (Gargamelle), Phys. Rev. Lett. **52**, 1096 (1984).
[4] P. Marage *et al.* (BEBC WA59), Z. Phys. C **31**, 191 (1986).
[5] H. J. Grabosch *et al.* (SKAT), Z. Phys. C **31**, 203 (1986).
[6] P. P. Allport *et al.* (BEBC WA59), Z. Phys. C **43**, 523 (1989).
[7] S. Willocq *et al.* (E632), Phys. Rev. D **47**, 2661 (1993).
[8] P. Vilain *et al.* (CHARM-II), Phys. Lett. B **313**, 267 (1993).
[9] M. Hasegawa *et al.* (K2K), Phys. Rev. Lett. **95**, 252301 (2005).
[10] D. Rein and L. M. Sehgal, Nucl. Phys. **B223**, 29 (1983).
[11] E. A. Paschos and A. V. Kartavtsev, hep-ph/0309148.
[12] A. A. Belkov and B. Z. Kopeliovich, Sov. J. Nucl. Phys. **46**, 499 (1987).
[13] B. Z. Kopeliovich, Nucl. Phys. B, Proc. Suppl. **139**, 219 (2005).
[14] S. S. Gershtein, Y. Y. Komachenko, and M. Y. Khlopov, Sov. J. Nucl. Phys. **32**, 861 (1980).
[15] Y. Y. Komachenko and M. Y. Khlopov, Yad. Fiz. **45**, 467 (1987).
[16] N. G. Kelkar, E. Oset, and P. Fernandez de Cordoba, Phys. Rev. C **55**, 1964 (1997).
[17] S. L. Adler, Phys. Rev. **135**, B963 (1964).
[18] J. D. Bjorken and E. A. Paschos, Phys. Rev. D **1**, 3151 (1970).
[19] Since $Q^2 > 0$, the $\lambda = 0$ polarization vector in (5) is timelike, while all other vectors in (4) and (5) are spacelike. Because of this the form of the closure condition becomes
- $$\sum_{\lambda=0, \pm 1} (-1)^\lambda \epsilon^\mu(\lambda) \epsilon^{\nu*}(\lambda) - \epsilon_t^\mu \epsilon_t^\nu = g^{\mu\nu}$$
- which is important in determining the sign of the \tilde{L}_{10} term in (6).

- [20] In principle we could insert here some pole contribution from the $a_1(1260)$ axial-vector boson, in order to describe possible Q^2 dependence in \mathcal{R}^ρ ; but this resonance is so far away from the relevant Q^2 region, that such an effort does not seem useful.
- [21] M. L. Goldberger and S. B. Treiman, *Phys. Rev.* **110**, 1178 (1958).
- [22] See e.g. also at C. Itzykson and J.-B. Zuber, *Quantum Field Theory* (McGraw-Hill, New York, 1980), p. 535, particularly the remark immediately after equation (11–113).
- [23] S. L. Adler, hep-ph/0505177.
- [24] B. Krusche *et al.*, *Eur. Phys. J. A* **22**, 277 (2004); nucl-ex/0406002; B. Krusche, “Photoproduction of Mesons Off Nuclei,” prepared for The 32nd International Workshop on Gross Properties of Nuclei and Nuclear Excitation, Hirschegg, Austria, 2004. Published in Hirschegg 2004, available through QSPIRES.
- [25] F. Binon *et al.*, *Nucl. Phys.* **B17**, 168 (1970).
- [26] G. Kahirmanis *et al.*, *Phys. Rev. C* **55**, 2533 (1997).
- [27] M. L. Scott *et al.*, *Phys. Rev. Lett.* **28**, 1209 (1972).
- [28] D. Ashery *et al.*, *Phys. Rev. C* **23**, 2173 (1981).
- [29] W. T. Meyer *et al.*, *Phys. Rev. Lett.* **28**, 1344 (1972).
- [30] F. Binon *et al.*, *Nucl. Phys.* **B33**, 42 (1971).
- [31] O. Bartholomy *et al.*, *Phys. Rev. Lett.* **94**, 012003 (2005).
- [32] J. J. Sakurai, *Currents and Mesons* (University of Chicago Press, Chicago, 1969).
- [33] J. Ballam *et al.*, *Phys. Rev. Lett.* **21**, 934 (1968).
- [34] R. Anderson *et al.*, *Phys. Rev. D* **1**, 27 (1970).
- [35] M. Guidal, J. M. Laget, and M. Vanderhaeghen, *Nucl. Phys.* **A627**, 645 (1997).
- [36] J. Breitweg *et al.* (ZEUS), *Eur. Phys. J. C* **12**, 393 (2000).
- [37] S. Chekanov *et al.* (ZEUS), *Nucl. Phys.* **B718**, 3 (2005).
- [38] We mention that for $\xi = 1$ the cross section is substantially bigger. For $E_1 = 1.3$ GeV it is 7.6×10^{-40} cm², which is still smaller than the experimental upper bound (25). At higher values of E_1 the cross section is approximately 1.5 to 2 times bigger.
- [39] D. Rein and L. M. Sehgal, hep-ph/0606185.
- [40] J. L. Raaf, PhD thesis, MiniBoone [Fermilab-Report No. 2005-20, 2005 (unpublished)].